Performance comparison of autothermal reforming for liquid hydrocarbons, gasoline and diesel for fuel cell applications

Inyong Kang, Joongmyeon Bae [*], Gyujong Bae

Department of Mechanical Engineering, Korea Advanced Institute of Science and Technology (KAIST), Daejeon, South Korea

Abstract

This paper discusses the reforming of liquid hydrocarbons to produce hydrogen for fuel cell applications, focusing on gasoline and diesel due to their high hydrogen density and well-established infrastructures. Gasoline and diesel are composed of numerous hydrocarbon species including paraffins, olefins, cycloparaffins, and aromatics. We have investigated the reforming characteristics of several representative liquid hydrocarbons. In the case of paraffin reforming, H_2 yield and reforming efficiency were close to thermodynamic equilibrium status (TES), although heavier hydrocarbons required slightly higher temperatures than lighter hydrocarbons. However, the conversion efficiency was much lower for aromatics than paraffins with similar carbon number. We have also investigated the reforming performance of simulated commercial diesel and gasoline using simple synthetic diesel and gasoline compositions. Reforming performances of our formulations were in good agreement with those of commercial fuels. In addition, the reforming of gas to liquid (GTL) resulted in high H_2 yield and reforming efficiency showing promise for possible fuel cell applications.
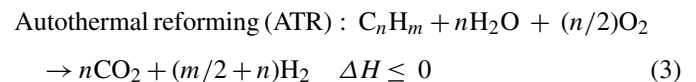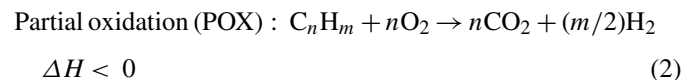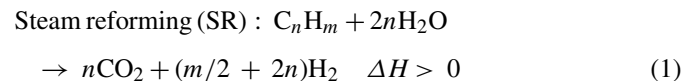© 2006 Elsevier B.V. All rights reserved.

Keywords: Fuel cell; Hydrogen; Autothermal reforming; Diesel; Gasoline; Liquid hydrocarbons

1. General autothermal reforming of gasoline and diesel

The high energy density and existing refueling infrastructure of petroleum-derived liquid hydrocarbon fuels, such as gasoline and diesel, have made them popular in all areas of industrial applications [1]. They are considered to be excellent candidate fuels for the production of hydrogen for fuel cell applications with compact fuel reformers [2]. Therefore, gasoline and diesel were studied extensively for the generation of hydrogen.

Catalytic autothermal reforming (ATR) of hydrocarbon fuels was first proposed by Argonne National Laboratory (ANL) and has been widely accepted as the most promising route to meet the efficiency, volume, and cost goals of the DOE fuel cell program [3,4]. As expressed below, ATR is a combination of partial oxidation (POX) and steam reforming (SR). An internal heat source supplied by POX leads to endothermic SR. Therefore, the ATR reaction can start quickly and stand alone without an additional heat supply, which makes it possible to construct a compact reformer [4–7].

Steam reforming (SR) : $C_nH_m + 2nH_2O$
$$\rightarrow nCO_2 + (m/2 + 2n)H_2 \quad \Delta H > 0 \tag{1}$$

Partial oxidation (POX) : $C_nH_m + nO_2 \rightarrow nCO_2 + (m/2)H_2$
$$\Delta H < 0 \tag{2}$$

Autothermal reforming (ATR) : $C_nH_m + nH_2O + (n/2)O_2$
$$\rightarrow nCO_2 + (m/2 + n)H_2 \quad \Delta H \leq 0 \tag{3}$$

There are also several disadvantages of ATR for liquid hydrocarbons. Hot spots can form easily due to the relative difference of reaction rates between POX and SR [8,9], which may cause degradation of the reforming catalyst. Heavier hydrocarbons, such as isooctane and hexadecane, are easily decomposed by thermal cracking during ATR and have a high possibility of coke formation [10]. Gasoline and diesel contain various aromatic compounds which have a higher tendency of coke formation than paraffinic fuels [11]. In addition, gasoline and diesel contain sul-

---

* Corresponding author. Tel.: +82 42 869 3045; fax: +82 42 869 8207.
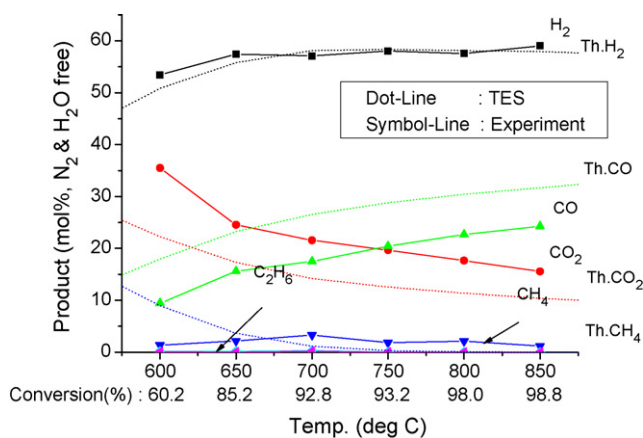*E-mail address:* jmbae@kaist.ac.kr (J. Bae).

Fig. 1. Product distribution of C_8H_{18} reforming ($C_8H_{18} = 0.076\,ml\,min^{-1}$, $H_2O/C = 1.25$, $O_2/C = 0.5$, CGO-Pt 0.5 wt.%, GHSV = $5000\,h^{-1}$).

Fig. 2. Product distribution of $C_{16}H_{34}$ reforming ($C_{16}H_{34} = 0.068\,ml\,min^{-1}$, $H_2O/C = 1.25$, $O_2/C = 0.5$, CGO-Pt 0.5 wt.%, GHSV = $5000\,h^{-1}$).

fur compounds and rapid degradation of catalyst performance by sulfur poisoning has been well-established [2,5,10,12–15].

Large efforts are required to improve reformer performance. Argonne National Laboratory (U.S.A) developed excellent catalysts with high performance for the ATR reaction. Their catalyst formulations have several resemblances to SOFC materials. For example, gadolinium-doped CeO_2 (CGO), which is used as a substrate for metal catalysts, is a good candidate for the electrolyte in low temperature-operating SOFC. Pt on CGO, which was patented by ANL, has shown higher reforming efficiency than commercial reforming catalysts made by several companies [8]. This can be explained by the redox mechanism of oxygen vacancies in CGO [3]. ANL has also investigated other various catalysts for the ATR of hydrocarbons. In the case of isooctane, precious metals, such as Pt (platinum) and Rh (rhodium), show higher performance than non-precious metals, such as Co (cobalt) and Ni (nickel). Pt and Rh showed similar performance at temperatures greater than 700 °C, but at lower temperatures, Rh has a better H_2 selectivity than Pt [3].

ATR reactions of gasoline and diesel using pellet-type catalysts are not reaction limited but mass transfer limited at high gas space velocities. They have fabricated a structured microchannel ATR catalyst with high performance, using Gd-doped CeO_2 with 0.5 wt.% Pt (CGO-Pt). Therefore, a reactor using a structured catalyst would be smaller and require less catalyst than a reactor using a pelletized catalyst [16–18].

2. A preliminary study

In a preliminary study [8], ATR of gasoline and diesel was conducted. C_8H_{18} (isooctane, 2,2,4-trimethylpentane—branched C_8) and $C_{16}H_{34}$ (hexadecane) were chosen as surrogate fuels for gasoline and diesel, respectively. C_8H_{18} is a typical simulant of gasoline [19]. $C_{16}H_{34}$ is the most predominant hydrocarbon in certified grade diesel fuel (38.7 wt.%) and aromatic fuels were included at 16.3 wt.%. The chemical expression of diesel was $C_{13.4}H_{26.3}$ [20].

Product distributions of C_8H_{18} and $C_{16}H_{34}$ reforming are shown in Figs. 1 and 2. Dotted-lines represent thermodynamic equilibrium status (TES) and solid lines with symbols are experi-
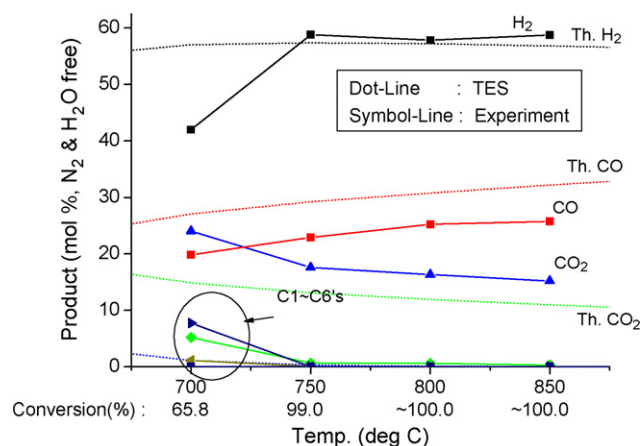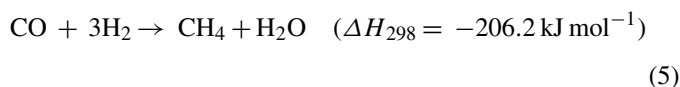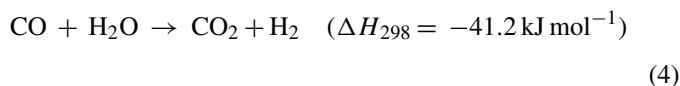
mental results. Under the conditions of the idealized autothermal reaction, the hydrocarbon is stoichiometrically converted into H_2 and CO_2 according to (3). In practice, however, this idealized chemistry is not attained because of the co-existence of other chemical reactions (the reverse water-gas shift reaction, methanation, incomplete conversion, etc.) [1]. As a result, the reformate typically contains CO, CH_4, and other species not included in (3). The kinetics of these other reactions are often fast enough that the reformate composition approaches thermodynamic equilibrium at the ATR reaction conditions [1]. The product distribution of C_8H_{18} reforming was obtained under the following conditions: $H_2O/C = 1.25$, $O_2/C = 0.5$, and gas hourly space velocity (GHSV) = $5000\,h^{-1}$ (Fig. 1). The experimental H_2 selectivity is very similar to TES and the fuel conversion is greater than 90% above 700 °C. The fuel conversion was defined as (# of carbons of CO, CO_2, CH_4 in the reformate gas)/(# of carbons in fuel injected) [8]. The H_2 yield of $C_{16}H_{34}$ reforming also approaches TES and almost 100% fuel conversion was attained above 750 °C (Fig. 2).

For the study of diesel reforming, $C_{12}H_{26}$ (dodecane) and $C_{16}H_{34}$ (hexadecane) were used individually as surrogates for diesel fuels. $C_{16}H_{34}$ represents the paraffinic compounds at the highest concentration in low-sulfur diesel fuel. The overall composition and heat of combustion of typical diesel fuel, however, are more closely represented by dodecane. The thermodynamic properties of a single hydrocarbon are well defined and can be calculated readily [1]. In the case of $C_{16}H_{34}$ reforming, the H_2 concentration is also in good agreement with TES at temperatures greater than 750 °C where fuel conversion is close to 100%. The CO yield is lower than TES while the CO_2 yield is higher than TES (Figs. 1 and 2). Generally, autothermal reforming reactions of hydrocarbons (C_nH_m) include the following reactions, (4) and (5), as well as (1) and (2) [21].
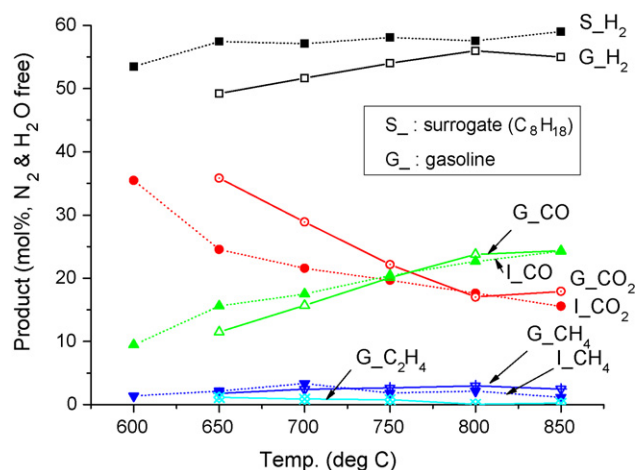
$$CO + H_2O \rightarrow CO_2 + H_2 \quad (\Delta H_{298} = -41.2\,kJ\,mol^{-1})$$

$$(4)$$

$$CO + 3H_2 \rightarrow CH_4 + H_2O \quad (\Delta H_{298} = -206.2\,kJ\,mol^{-1})$$

$$(5)$$

Fig. 3. Comparison of product distribution of gasoline and C_8H_{18} (H_2O/C = 1.25, O_2/C = 0.5, CGO-Pt 0.5 wt.%, GHSV = 5000 h^{-1}).

The heat required for the endothermic steam reforming (1) is supplied by the partial oxidation (2). The shift reaction (4) and the methanation reaction (5) proceed simultaneously and yield a gas composition which corresponds to TES. But CGO-Pt showed high selectivity for the shift reaction (4) when H_2O was added [8], causing deviations of CO and CO_2 from TES.

From the basis of these results, commercial gasoline and diesel reforming were conducted at the same conditions. Figs. 3 and 4 present product distributions obtained by commercial fuels (gasoline, diesel) and surrogate fuels (C_8H_{18}, $C_{16}H_{34}$), respectively.

In Fig. 3, solid lines with symbols represent the product distribution from C_8H_{18} reforming and dotted lines with symbols represent the product compositions from gasoline reforming. Over the entire range of temperature, H_2 yields obtained from gasoline reforming are not as high as C_8H_{18} reforming. In addition, there are some differences between the product yields of gasoline and C_8H_{18} reforming. Diesel also has different product yields from the surrogate fuel, $C_{16}H_{34}$. However, the difference between the reforming results of diesel and $C_{16}H_{34}$ is greater than that of gasoline. The H_2 obtained in diesel reforming
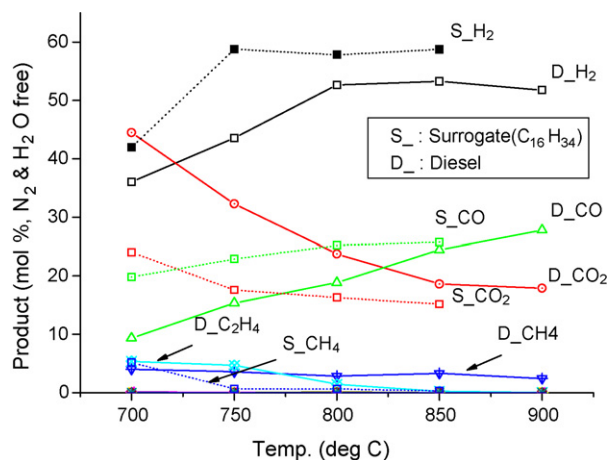

Fig. 4. Comparison of product distribution of diesel and $C_{16}H_{34}$ [8] (H_2O/C = 1.25, O_2/C = 0.5, CGO-Pt 0.5 wt.%, GHSV = 5000 h^{-1}).

Table 1
Liquid hydrocarbons used for autothermal reforming

Fuels	Provider	Features
Hexadecane ($C_{16}H_{34}$)	Sigma–Aldrich	>99%
Dodecane ($C_{12}H_{26}$)	Sigma–Aldrich	>99%
1-Methyl naphthalene	Sigma–Aldrich	>95%, HPLC grade
Isooctane (C_8H_{18})	Sigma–Aldrich	>99.7%, HPLC grade
Toluene (C_7H_8)	Sigma–Aldrich	>99.8%, HPLC grade
Hexane (C_6H_{14})	Sigma–Aldrich	>95%, HPLC grade
Cyclo-hexane (C_6H_{12})	Sigma–Aldrich	>99.9%, HPLC grade
MTBE	Sigma–Aldrich	>99.8%, HPLC grade
Diesel	LG Caltex Oil	Commercial diesel
Gasoline	SK Oil	Commercial gasoline
GTL diesel	Shell Korea	Commercial GTL diesel

never approaches the H_2 yield obtained from $C_{16}H_{34}$ reforming. Unreacted hydrocarbons produced by $C_{16}H_{34}$ reforming are negligibly diminished, but diesel reforming has an average CH_4 concentration of 3%.

We found that the reforming performance of the surrogates was very different from the commercial fuels. Therefore, it is difficult to represent commercial fuels with only a single component because gasoline and diesel fuels are hydrocarbon mixtures containing alkanes, alkenes, and aromatics. Diesel with a boiling range between 200 and 380 °C consists of several hundred different compounds [21]. Aromatics are known to slow the reforming kinetics and to increase carbon formation [19]. In this study, a more detailed investigation of hydrocarbon reforming was conducted.

3. Experiment

3.1. Experimental setup

The variety of liquid hydrocarbons and commercial fuels that were studied are listed in Table 1. Air and vaporized water were added with the fuel into the reactor. Fuel and water were injected with HPLC pumps (MOLEH Co., Ltd.), while air was injected and controlled with a mass flow controller (MKS). Ultra Pure (>10 MΩ) water was used. An external heat exchanger was installed to vaporize the water and the vaporized water was carried by N_2. The reactor temperature was controlled by an electric furnace. Product gases were analyzed by a GC–MS (Agilent 6890N) after a moisture removal procedure. Operating conditions were determined by the preliminary study [8]. Pressure, O_2/C, H_2O/C, and GHSV were 1 bar, 0.5, 1.25, and 5000 h^{-1}, respectively.

3.2. Reactor

Two k-type thermocouples were installed at the top and the bottom of the catalyst bed. CGO-Pt 0.5 wt.% was used as the reforming catalyst. Fine powders of CGO-Pt 0.5 wt.% were prepared by the combustion method. After the catalysts were pelletized, they were crushed into granules (~500 μm). Packed-bed-typed reactors were used for these experiments.

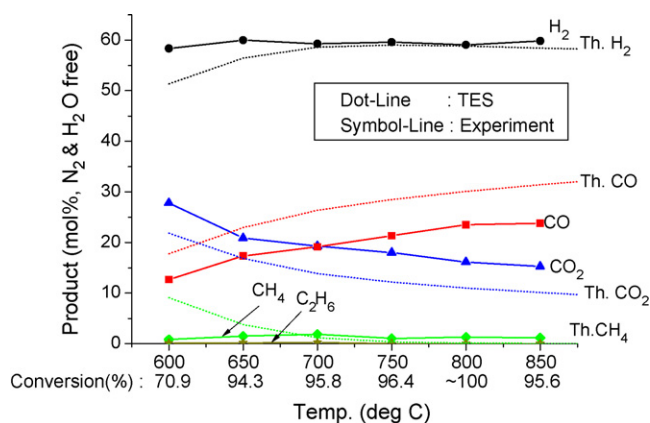Fig. 5. Product distribution of C_6H_{14} reforming ($C_6H_{14} = 0.079\,\text{ml min}^{-1}$, $H_2O/C = 1.25$, $O_2/C = 0.5$, CGO-Pt 0.5 wt.%, GHSV = 5000 h^{-1}).
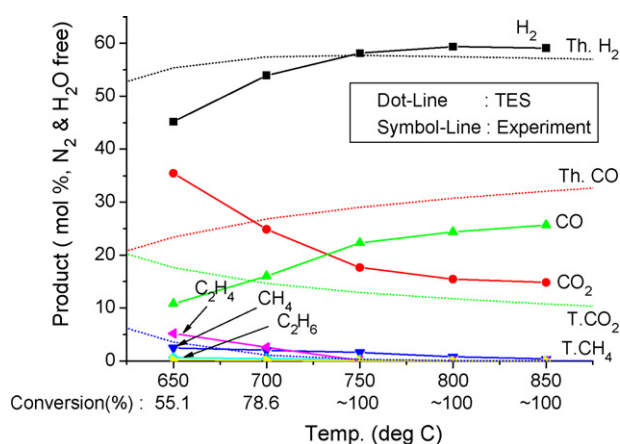
Fig. 6. Product distribution of $C_{12}H_{26}$ reforming ($C_{12}H_{26} = 0.070\,\text{ml min}^{-1}$, $H_2O/C = 1.25$, $O_2/C = 0.5$, CGO-Pt 0.5 wt.%, GHSV = 5000 h^{-1}).

3.3. Experimental result and discussion

3.3.1. Paraffinic hydrocarbons reforming

The product distribution of C_6H_{14} (normal hexane) and $C_{12}H_{26}$ (dodecane) reforming are shown in Figs. 5 and 6, respectively. Dotted lines and solid lines with symbols show the results of TES and experiment, respectively. Fuel conversions at each temperature are listed under the *x*-axis.

Where,

$$\text{fuel conversion (\%)} = \frac{\substack{\text{atomic carbon concentration of CO,} \\ \text{CO}_2, \text{ and CH}_4 \text{ in the reformate}}}{\text{atomic carbon concentration in the fuel}}$$

The fuel conversion increases with increasing temperature. C_6H_{14} reforming approaches 100% conversion at lower temperatures than $C_{12}H_{26}$. As previously explained, CO and CO_2 are both different from TES (Figs. 5 and 6).

Thus far, the reforming results of C_6H_{14}, C_8H_{18}, $C_{12}H_{26}$, and $C_{16}H_{34}$ have been presented. Table 2 lists the fuel conversions of each fuel at various temperatures. It is confirmed that higher hydrocarbons with longer chained structures demand higher temperatures to obtain fuel conversions greater than 90%. These results can explain how hydrocarbons are reformed. Larger hydrocarbons have lower C–C bond energies than smaller hydrocarbons [2]. Therefore, higher hydrocarbon reforming seems to be easier than lower hydrocarbon reforming because our reactor, which is temperature-controlled by an electrical furnace, can be considered as an infinite heat reservoir. This also shows that the decomposition of all C–C bonds does not happen simultaneously, but the transformation of higher hydrocarbons into lower hydrocarbons, such as aromatics and olefins, with higher C–C bond energies occurs. In practice, short chained paraffinic hydrocarbons tend to more favorable light-off and reforming characteristics for catalytic autothermal reforming than longer chained and aromatic components [19].

In the reforming of higher hydrocarbons, they are first adsorbed irreversibly onto metal sites and then C–C bond cleavage occurs one bond at a time until the hydrocarbons are converted into C_1 components. However, reaction rates of individual hydrocarbons on a given catalyst are often quite different. Higher hydrocarbons may also be converted into aromatic hydrocarbons due to their stable carbon structure, by catalytic active sites, and non-catalytic thermal cracking. Once aromatics are produced, it is difficult to remove them. In addition, they decrease the overall reaction rate [10,13,22]. The reforming results obtained using aromatic hydrocarbons will be discussed below.
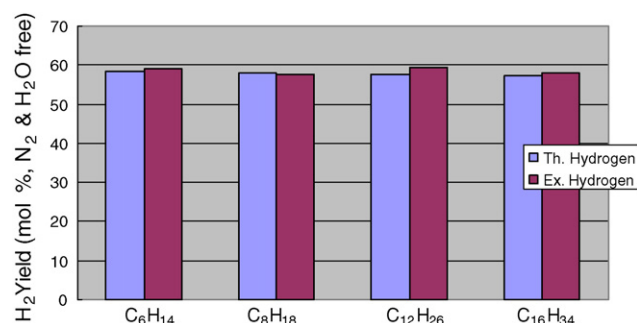

Fig. 7. H_2 yield for paraffinic hydrocarbons ($O_2/C = 0.5$, $H_2O/C = 1.25$, furnace temperature = 800 °C, CGO-Pt 0.5 wt.%, GHSV = 5000 h^{-1}).

Table 2
Fuel conversions according to temperature using paraffinic hydrocarbon (%)

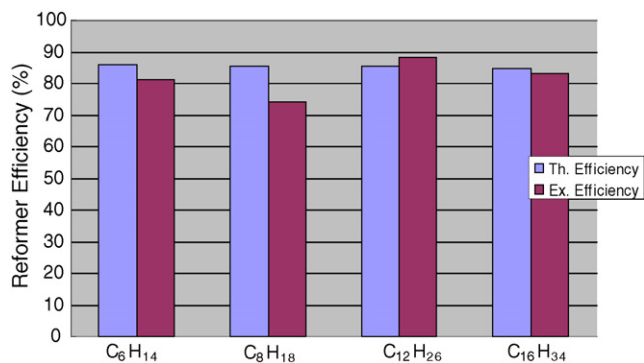|	T (°C)					
	600	650	700	750	800	850
Hexadecane ($C_{16}H_{34}$)			65.8	99.0	~100	~100
Dodecane ($C_{12}H_{26}$)		55.1	78.6	~100	~100	~100
Isooctane (C_8H_{18})	60.2	85.2	92.8	93.2	98.0	98.8
Hexane (C_6H_{14})	70.9	94.3	95.8	96.4	~100	95.6

Fig. 8. Reforming efficiency according to paraffinic hydrocarbon ($O_2/C = 0.5$, $H_2O/C = 1.25$, furnace temperature: 800 °C, CGO-Pt 0.5 wt.%, GHSV = 5000 h^{-1}).

Figs. 7 and 8 show the hydrogen yield and reforming efficiency of each paraffinic fuel. The H_2 yields are in good agreement with the values obtained by TES. Reforming efficiencies are also close to TES, even though individually they show slight deviations. Reforming reactions of paraffinic hydrocarbon were too rapid to reach TES.

Where, hydrogen yield = H_2 mole percent in product on the N_2 and H_2O free basis

$$\text{Reforming efficiency} = \frac{\text{LHV of } H_2 \text{ and CO in the reformate}}{\text{LHV of the fuel}}.$$

3.3.2. Reforming performance for different carbon structures

The importance of the carbon structure for reforming is well known with respect to the reforming energy exhausted and the long-term performance of the reformer which is affected by carbon formation. In our study, we have investigated a few hydrocarbons with different carbon structures. C_6H_{14} (n-hexane), C_6H_{12} (cyclo-hexane), C_7H_8 (toluene), and $C_{11}H_{10}$ (1-methyl-naphthalene) were used.

The product yields from C_6H_{12} reforming are shown in Fig. 9. The H_2 yield is in good agreement with TES and the fuel con-
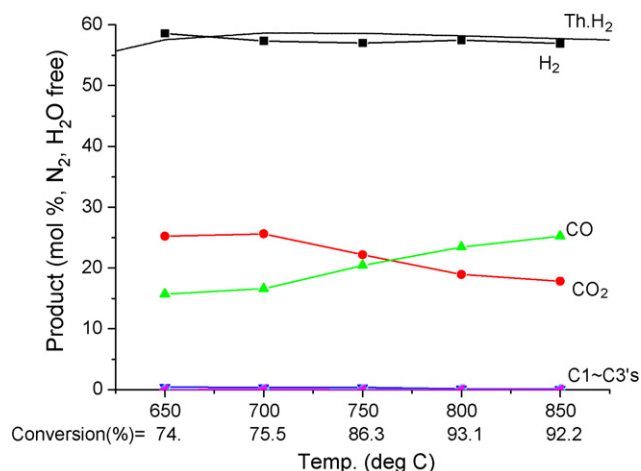
version is greater than 90% at 800 °C. The reforming results of other types of hydrocarbons, mono-aromatic (C_7H_8) and poly-aromatic ($C_{11}H_{10}$) are shown in Figs. 10 and 11. Both have low fuel conversion at most temperatures. $C_{11}H_{10}$ could not reach 90% fuel conversion, even at 850 °C and seemed to be the most difficult fuel to reform.

Fuel conversions for different carbon structures are shown in Table 3. It is confirmed that fuel conversions greater than 90% are more difficult to obtain with increasing aromaticity of the fuel. Table 4 shows the physical properties of the various hydrocarbons. C_6H_{14}, C_6H_{12}, and C_7H_8 have similar molar mass, but have very different carbon structures as shown in Fig. 12.

Boiling points of each fuel are associated with the difference of carbon structure. According to Tables 3 and 4, hydrocarbons with higher boiling points demand more energy for reforming. Generally C–C bond energies of aromatics are stronger than that of paraffins, which decreases the reaction rate. The aromatic structure of the fuel is not readily oxidized or cleaved to yield lower carbon number species. The stability of the aromatic ring makes such fuels more difficult to reform than the branched paraffinic fuels [18].
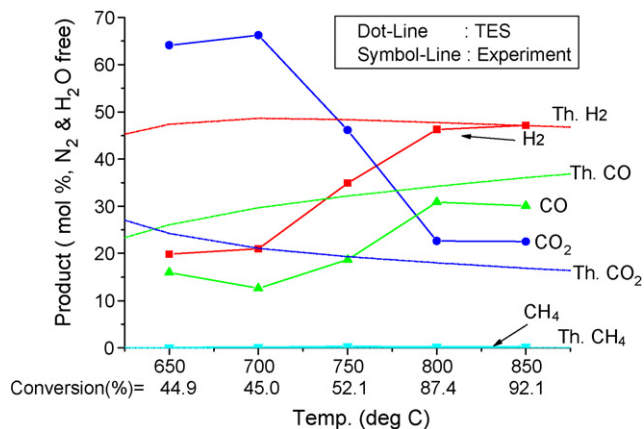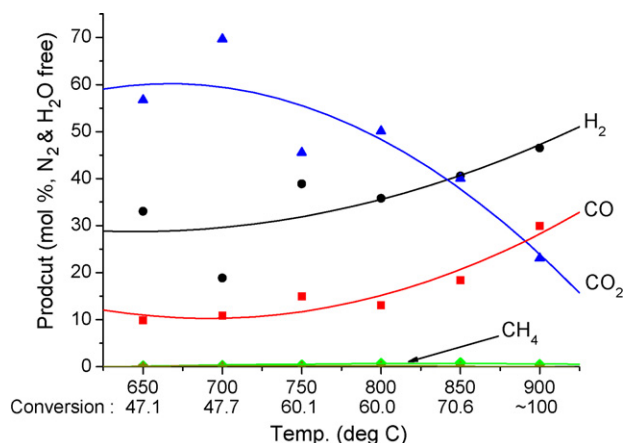

Fig. 10. Product distribution of C_7H_8 (toluene) reforming ($C_7H_8 = 0.056$ ml min^{-1}, $H_2O/C = 1.25$, $O_2/C = 0.5$, CGO-Pt 0.5 wt.%, GHSV = 5000 h^{-1}).

Fig. 9. Product distribution of C_6H_{12} reforming ($C_6H_{12} = 0.065$ ml min^{-1}, $H_2O/C = 7.5$, $O_2/C = 3$, CGO-Pt 0.5 wt.%, GHSV = 5000 h^{-1}).

Fig. 11. Product distribution of $C_{11}H_{10}$ reforming ($C_{11}H_{10} = 0.048$ ml min^{-1}, $H_2O/C = 1.25$, $O_2/C = 0.5$, CGO-Pt 0.5 wt.%, GHSV = 5000 h^{-1}).

Table 3
Fuel conversion (%) for different carbon structures

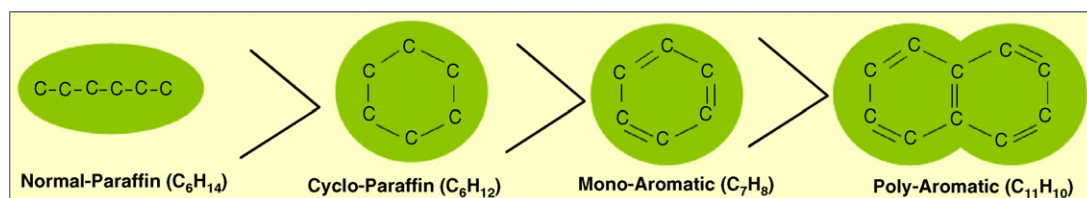|	T (°C)					
	600	650	700	750	800	850
Hexane (C_6H_{14})	70.9	94.3	95.8	96.4	~100	95.6
Cyclohexane (C_6H_{12})		74.2	75.5	86.3	93.1	92.2
Toluene (C_7H_8)		44.9	45.0	52.1	87.4	92.1
Methylnaphthalene ($C_{11}H_{10}$)			47.7	60.1	60.0	70.65

Fig. 12. Carbon structures of hydrocarbons.

C_6H_{12} is a cycloparaffin that has a similar carbon structure to benzene. Its degree of reforming seems to be between C_6H_{14} and C_7H_8. Olefins are known as precursors for carbon formation and are produced in the process of thermal cracking or pyrolysis of the higher hydrocarbons. In particular, ethylene leads to rapid carbon formation [13]. Olefinic compounds can easily degrade to carbon either in the gas phase at the higher temperatures, or on the catalyst/support surfaces at high and intermediate temperatures [22]. $C_{11}H_{10}$ has a poly-aromatic structure as described (Fig. 12). Its conversion efficiency is lower than any other hydrocarbon used in our study. Although there are many factors that determine the reforming performance, we can summarize the reforming performance of the different hydrocarbons, at the same conditions with respect to fuel conversion, as shown below.

$C_{11}H_{10}$ (poly-aromatic) $< C_7H_8$ (mono-aromatic) $< C_6H_{12}$ (cyclo-paraffin) $< C_6H_{14}$ (saturated paraffin).

In the case of liquid hydrocarbon reforming, obtaining higher fuel conversions is very important. If the fuel conversion is low, hydrocarbon breakthrough occurs. Hydrocarbons in the reformate gas not only reduce the reforming efficiency, but they can affect degradation of water-gas shift and preferential CO oxidation catalysts [3]. This concern is not just a question of catalytic activity, but it relates to the design of the fuel processor. Ideally, fuel, air, and steam would be mixed homogeneously in the gas phase before being exposed to the catalyst. In reality, the mixture will be exposed to hot surfaces before reaching the catalyst, which may lead to pre-ignition or thermal decomposition [3].

Krumpelt et al. [3] suggests that hydrocarbon breakthrough is not related to a catalytic reaction. They prepared three types of

catalysts, including silicon carbide, CGO-20, and Pt/CGO-20. Silicon carbide is known as typical inert material. After C_8H_{18} autothermal reforming over SiC, CO, CO_2, C_3's, C_4's, C_6H_6, and unconverted C_8H_{18} were formed due to thermal decomposition from the gas phase reaction, but no H_2 was generated. In the case of CGO-20, H_2, CO, CO_2, C_3's, C_4's, C_5's, C_6H_6, and unconverted C_8H_{18} were produced after C_8H_{18} reforming. Unlike silicon carbide C_3's, C_4's, and C_5's were decreased above 700 °C, suggesting the existence of other surface reactions. In the case of Pt/CGO-20, most of the hydrocarbons, except CH_4 and C_6H_6, disappeared with increasing temperature.

C_6H_6 is not produced catalytically, but through gas phase reactions. Once aromatic hydrocarbons are formed, it is difficult to remove them by catalytic processes [3]. Similar results have already been presented by Flytzani-Stephanopoulos and Voecks [22]. They monitored the concentration of C_6H_6 and it did not disappear along the catalyst bed

H_2 yield and reforming efficiency for different carbon structures are shown in Figs. 13 and 14. H_2 yields of aromatic hydrocarbons were slightly lower than that of paraffins with respect to TES. The H_2 yield of $C_{11}H_{10}$ had especially large
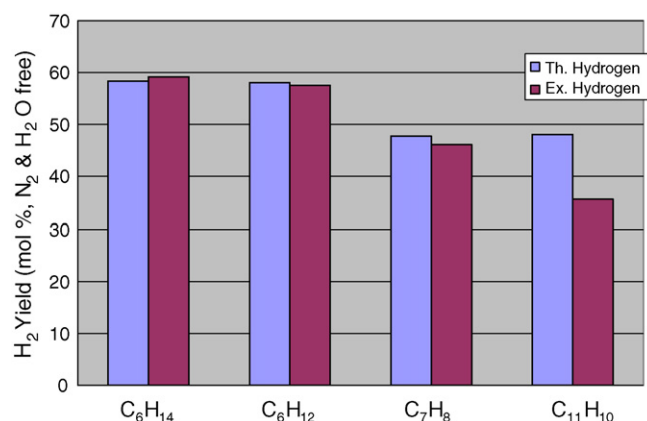
Table 4
Physical properties of hydrocarbon fuels

	Density (g ml^{-1})	Mol. wt. (g mol^{-1})	Boiling point (K)
C_6H_{14}	0.655	86.18	341.90
C_6H_{12}	0.779	84.16	353.90
C_7H_8	0.867	92.14	383.80
$C_{11}H_{10}$	1.020	142.20	517.90

Fig. 13. H_2 yield for different carbon structures (O_2/C = 0.5, H_2O/C = 1.25, furnace temperature = 800 °C, CGO-Pt 0.5 wt.%, GHSV = 5000 h^{-1}).
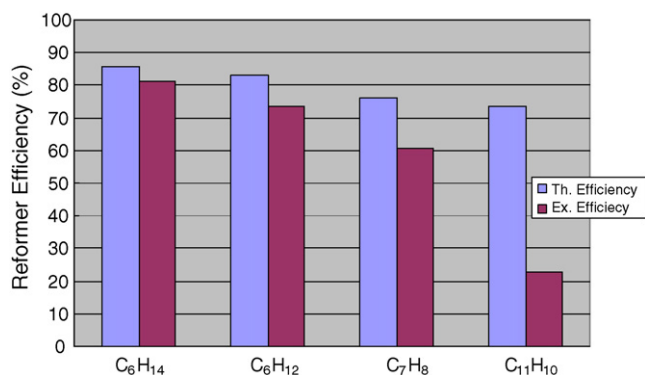
Fig. 14. Reforming efficiency (%) ($O_2/C = 0.5$, $H_2O/C = 1.25$, furnace temperature = 800 °C, CGO-Pt 0.5 wt.%, GHSV = 5000 h^{-1}).

differences from TES. The reforming efficiency of aromatics decreases dramatically causing an increase in the differences of experimental data from TES data (Fig. 13). These results are in agreement with those published by Palm et al. [21]. Aromatic hydrocarbons show lower reforming kinetics than paraffins.

3.3.3. Simulated gasoline and diesel

Commercial fuels such as gasoline and diesel consist of a variety of hydrocarbon fuels. Therefore, it is impossible to represent them with a single hydrocarbon. As mentioned in the introduction, there were large differences in the reforming performance between surrogate fuels and commercial fuels. On the basis of hydrocarbon reforming, we could synthesize simulated gasoline and diesel.

Generally simulated fuels are composed of paraffinic hydrocarbons and aromatic hydrocarbons.

Our composition of simulated gasoline is 80% paraffins and 20% aromatics with respect to volume. The specific composition is shown below [23]:

Isooctane (C_8H_{18}) : 50 vol%   hexane (C_6H_{14}) : 20 vol%

Toluene (C_7H_8) : 20 vol%   MTBE ($C_5H_{12}O$) : 10 vol%

The product distribution of synthetic gasoline is in good agreement with commercial gasoline (Fig. 15). Table 5 shows the physical properties of the synthetic and commercial fuels.

We could synthesize our own simulated diesel in the light of ANL's composition [25]. Generally, the composition of diesel is more complex than gasoline including hundreds of hydrocarbons, and making it very difficult to simulate commercial diesel. According to reference [14], jet fuel, which has similar features to diesel, has 14–20% aromatic hydrocarbons and their simulated jet fuel is described as $C_{11.9}H_{22.8}$.
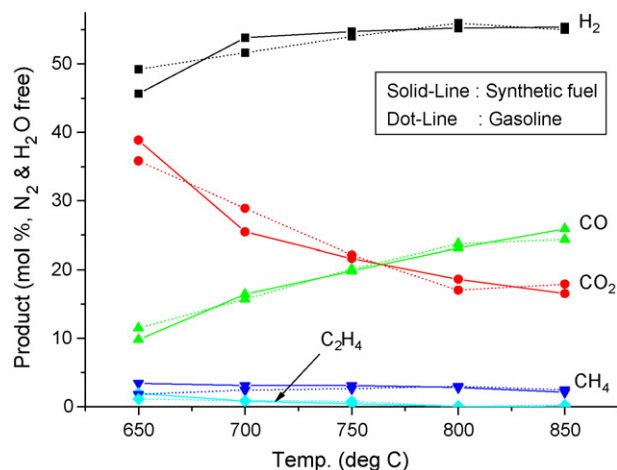

Fig. 15. Product distribution of synthetic and commercial gasoline ($H_2O/C = 1.25$, $O_2/C = 0.5$, CGO-Pt 0.5 wt.%, GHSV = 5000 h^{-1}).
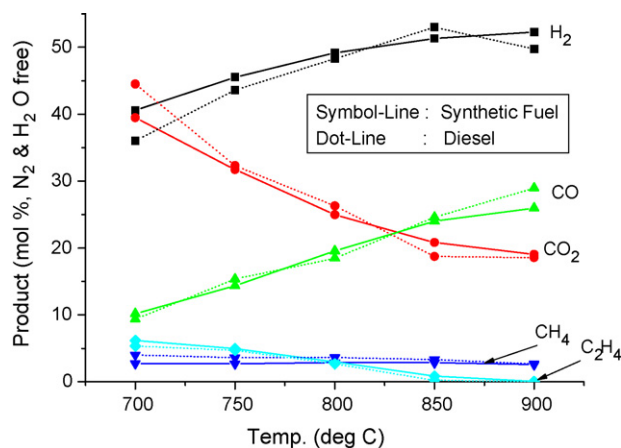

Fig. 16. Product distribution of synthetic and commercial diesel ($H_2O/C = 1.25$, $O_2/C = 0.5$, CGO-Pt 0.5 wt.%, GHSV = 5000 h^{-1}).

We have tried to find more simple formulations to make calculations such as fuel conversion, O_2/C, and H_2O/C less cumbersome. Unlike reference [2], we have used only two components to simulate diesel. The representative paraffin and aromatic were $C_{12}H_{26}$ (dodecane) and $C_{11}H_{10}$ (methyl naphthalene), respectively. Synthetic fuel is in very good agreement with commercial diesel (Fig. 16). Physical properties of the fuels are listed in Table 6.

$C_{12}H_{26}$ (dodecane) : 70 vol%

$C_{11}H_{10}$ (methyl naphthalene) : 30 vol%

According to these results, the H_2 yield of paraffins decreased with the addition of aromatic fuels, showing similar results to

Table 5
Physical properties of synthetic and commercial gasoline [24]

Chemical expression	Mass (g mol^{-1})	Density (g ml^{-1})	LHV (MJ kg^{-1})	C/H/O (wt.%)
$C_{7.0}H_{13.9}O_{0.1}$	99.624	0.725	42.6	84/14/2
Gasoline	98	0.750	43.2	85/15/0

Table 6
Physical properties of synthetic and commercial diesel [24]

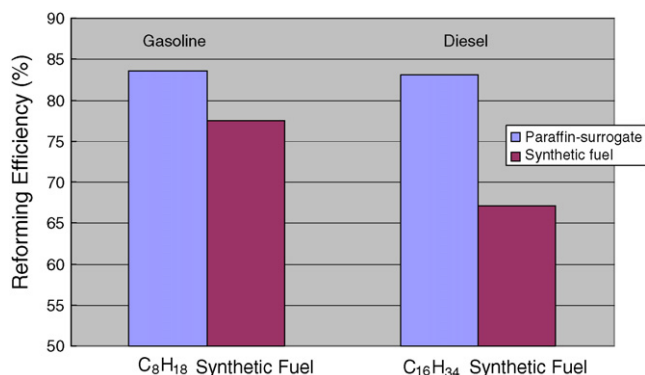| Chemical expression	Mass (g mol^{-1})	Density (g ml^{-1})	LHV (MJ kg^{-1})	C/H/O (wt.%)
$C_{11.6}H_{19.5}$	158.88	0.824	42.7	88/12/0
Diesel	170	0.831	42.7	86/14/0

Fig. 17. Reforming efficiency of gasoline and diesel ($H_2O/C = 1.25$, $O_2/C = 0.5$, furnace temperature $= 850\,°C$, GHSV $= 5000\,h^{-1}$).

the commercial fuels, gasoline and diesel. These results are in good agreement with reference [15].

The reforming efficiencies of surrogate fuels are compared with synthetic fuels in Fig. 17. There are large differences between the surrogate fuels and synthetic fuels, especially in the case of diesel which shows a severe efficiency drop.

Therefore, converting diesel fuel into a hydrogen-rich gas that is suitable for fuel cells is more challenging than converting gasoline because of the multi-cyclic aromatics and the aromatic sulfur compounds in diesel fuel. To break down these compounds, the operating temperature of the reformer must be raised and the reforming catalyst needs to be significantly tolerant to sulfur [26].

In addition, we have investigated gas to liquid (GTL) diesel, which is a candidate fuel for automobiles in the future. It has a small amount of aromatic compounds and sulfides and most
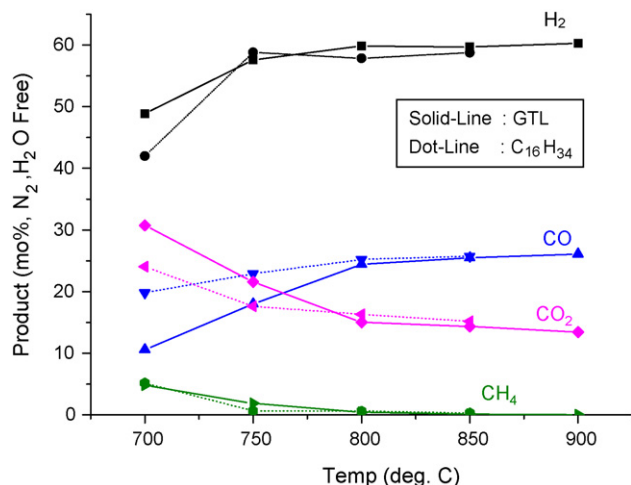

Fig. 18. Product distribution of $C_{16}H_{34}$ and GTL diesel ($H_2O/C = 1.25$, $O_2/C = 0.5$, CGO-Pt 0.5 wt.%, GHSV $= 5000\,h^{-1}$).
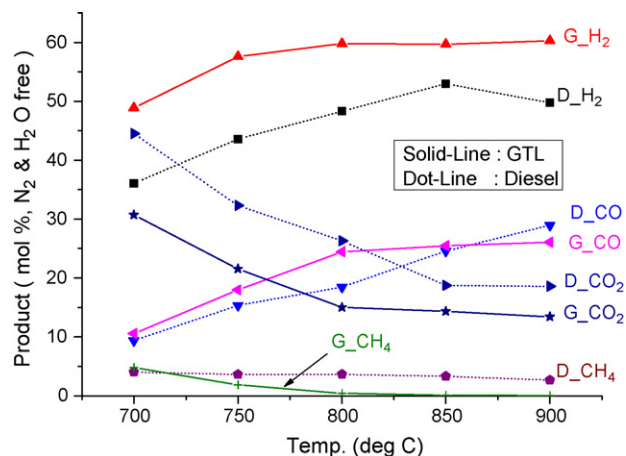

Fig. 19. Product distribution of GTL and diesel (op. conditions of synthetic diesel, $O_2/C = 0.5$, H_2O/C, CGO-Pt 0.5 wt.%, GHSV $= 5000\,h^{-1}$).
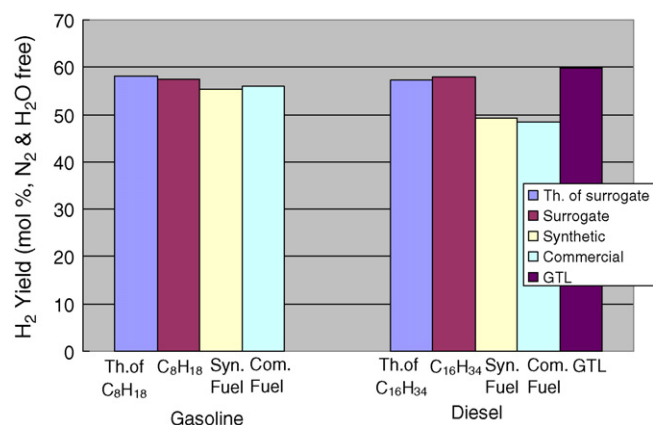

Fig. 20. H_2 yield of commercial fuels ($H_2O/C = 1.25$, $O_2/C = 0.5$, furnace temperature $= 800\,°C$, GHSV $= 5000\,h^{-1}$).

of the compounds are paraffinic hydrocarbons [27]. According to our studies, we predicted that the reforming performance of GTL would be similar to $C_{16}H_{34}$, which is one of the dominant hydrocarbons in diesel. GTL does show similar reforming performance with $C_{16}H_{34}$ as shown in Figs. 18 and 19. GTL has better reforming efficiency than diesel which is very interesting for fuel cells. GTL diesel not only has a high productivity of hydrogen, but also has a higher reforming efficiency than diesel. Therefore, GTL diesel shows the best performance (Fig. 20) and can be call fuel cell grade fuel.

4. Conclusion

We have investigated the reforming efficiency for a variety of hydrocarbons. Hydrocarbons can be classified as paraffinic

or aromatic. Aromatics have more stable structures than paraffins, which decreases reaction rates. In our studies, most paraffin fuels showed good performance, even though higher hydrocarbons required slightly higher temperatures. But aromatics have lower efficiency than paraffins at the same conditions and the reforming performance of poly-aromatics was the worst of all the hydrocarbons used.

On the basis of reforming performance for hydrocarbons, we can synthesize simulated fuels for gasoline and diesel. Their performances are in good agreement with commercial fuels. Aromatics in gasoline and diesel not only cause the lower reforming efficiency but the degradation of the catalysts in the shift reactor and preferential oxidation reactor, although this was not discussed previously. In addition, GTL diesel, which is mostly composed of paraffinic fuels with little aromatic and sulfides, shows good performance. GTL with high reforming efficiency could be considered a fuel cell grade fuel.

Acknowledgments

References

[1] D.-J. Liu, T.D. Kaun, H.-K. Liao, S. Ahmed, Int. J. Hydrogen Energy 29 (2004) 1035–1046.
[2] X. Ma, L. Sun, C. Song, Catal. Today 77 (2002) 107–116.
[3] M. Krumpelt, T. Krause, J.D. Carter, J. Mawdsley, J.-M. Bae, S. Ahmed, C. Rossignol, Catalytic Autothermal Reforming, 2001 DOE Annual Progress Report, Fuel Cells for Transportation.
[4] S. Ahmed, M. Kumpelt, Int. J. Hydrogen Energy 26 (2001) 291–301.
[5] P.K. Cheekatamarla, A.M. Lane, J. Power Sources 152 (2005) 157–164.
[6] S. Ayabe, H. Omoto, T. Utaka, R. Kikuchi, K. Sasaki, Y. Teraoka, K. Eguchi, Appl. Catal. A: Gen. 241 (2003) 261–269.
[7] S.H.D. Lee, D.V. Applegate, S. Ahmed, S.G. Calderone, T.L. Harvey, Int. J. Hydrogen Energy 30 (2005) 829–842.
[8] I. Kang, J. Bae, Autothermal reforming study of diesel for fuel cell application, J. Power Sources 159 (2006) 1283–1290.
[9] A. Qi, S. Wang, G. Fu, D. Wu, Appl. Catal. A: Gen. 293 (2005) 71–82.
[10] F. Joensen, J.R. Rostrup-Nielsen, J. Power Sources 105 (2002) 195–201.
[11] A. Shamsi, J.P. Baltrus, J.J. Spivey, Appl. Catal. 293 (2005) 145–152.
[12] P.K. Cheekatamarla, W.J. Thomson, Appl. Catal. A: Gen. 287 (2005) 176–182.
[13] J.R. Rostrup-Nielsen, I. Dybkjaer, T.S. Christensen, Stud. Surf. Sci. Catal. 113 (1998) 81.
[14] B. Lenz, T. Aicher, J. Power Sources 149 (2005) 44–52.
[15] C. Palm, P. Cremer, R. Peters, D. Stolten, J. Power Sources 106 (2002) 231–237.
[16] M. Krumpelt, J.D. Carter, R. Wilkenhoener, S.H.D. Lee, J.-M. Bae, S. Ahmed, 2000 Fuel Cell Seminar, October 2000, Portland, Oregon, 2000.
[17] J.-M. Bae, S. Ahmed, R. Kumar, E. Doss, J. Power Sources 139 (2005) 91–95.
[18] R. Ahluwalia, S. Ahmed, J.-M. Bae, J.D. Carter, E.D. Doss, J. Kopasz, T. Krause, J. Krebs, M. Krumpelt, R. Kumar, S.H.D. Lee, D. Myers, C. Pereira, X. Wang, Development of Fuel Processors for Polymer Electrolyte Fuel Cell Systems at Argonne National Laboratory, 1st European Polymer Electrolyte Fuel Cell Forum, Lucerne, Switzerland, July 2–6, 2001.
[19] R.L. Borup, M.A. Inbody, T.A. Semelsberger, J.I. Tafoya, D.R. Guidry, Catal. Today 99 (2005) 263–270.
[20] C. Pereira, J.-M. Bae, S. Ahmed, M. Krumpelt, Liquid Fuel Reformer Development: Autothermal Reforming of Diesel Fuel, Argonne National Laboratory Chemical Technology Division Argonne, IL 60439, 2001.
[21] C. Palm, P. Cremer, R. Peters, D. Stolten, J. Power Sources 106 (2002) 231–237.
[22] M. Flytzani-Stephanopoulos, G.E. Voecks, Int. J. Hydrogen Energy 7 (7) (1983) 539–548.
[23] Gasoline Composition of SK Corporation in Korea.
[24] Gasoline and Diesel Data Obtain by Engine Laboratory in Korea Institute of Science and Technology (KAIST).
[25] ANL's Composition of Diesel.
[26] M. Krumpelt, D.-J. Liu, Technology Development in Support of the Solid State Energy Conversion Alliance, Office of Fossil Energy Fuel Cell Program, FY 2004 Annual Report.
[27] R.H. Clack, J.J.J. Louis, R.J. Stradring, Shell Gas to Liquids in the Context of Future Engines and Future Fuels, Shell Global Solutions (UK).